Iranian Journal of Catalysis 9(1), 2019, 51-61

IRANIAN JOURNAL OF CATALYSIS

Kinetic comparison of Ni/Al_2O_3 and $Ni/MgO-Al_2O_3$ nano structure catalysts in CO_2 reforming of methane

Zahra Alipour[a], Fereshteh Meshkani[a,b,*], Mehran Rezaei[a,b]

[a]*Department of Chemical Engineering, University of Kashan, Km 6 Ravand Road, Kashan, Post Code: 87317-51167, Iran.*
[b]*Institute of Nano Science and Nano Technology, University of Kashan, Km 6 Ravand Road, Kashan, Post Code: 87317-51167, Iran.*

Received 4 November 2017; received in revised form 15 August 2018; accepted 25 September 2018

ABSTRACT

The kinetic characteristics of the Ni/Al_2O_3 and $Ni/MgO-Al_2O_3$ catalysts were investigated in CO_2 reforming of methane (CRM). The reaction orders (α and β) and the rate constant (k) were calculated using the non-linear regression analysis, in which the sum of the squared differences of calculated and experimental CO_2 reforming of methane rates were minimized. The acquired results demonstrate that the methane partial pressure has a significant influence on the reaction rate compared to the partial pressure of carbon dioxide in CRM and the reaction rate of MgO- modified catalyst was higher than the unmodified sample. This may be due to the higher catalytic activity of $Ni/MgO-Al_2O_3$ compared to that of Ni/Al_2O_3 in CRM. The activation energy for CH_4 consumption was higher than that of CO_2. Meanwhile, adding CO and H_2 to the feed has a negative effect on the reaction rate. The experimental CH_4 consumption rates for both Ni/Al_2O_3 and $Ni/Mg-Al_2O_3$ were fitted to some kinetic type models in order to investigate the effect of MgO modifier on the reaction kinetics of the Ni catalyst so the model with the lowest squared error was proposed as the best model describing the reaction rate.

Keywords: *Ni catalysts, CO_2 reforming of methane, Kinetics, Synthesis gas.*

1. Introduction

The production of synthesis gas via the dry reforming reaction is of great importance due to the industrial and environmental aspects. This process uses the CH_4 and CO_2 as feedstocks, which are greenhouse gases [1-3]. The synthesis gas produced by the dry reforming reaction has a lower H_2/CO molar ratio, compared to other syngas production methods such as steam reforming and partial oxidation of methane. The produced syngas in this process can be employed for the production of valuable oxygenated chemicals and liquid hydrocarbons [1,4-6].

$$CH_4 + CO_2 \rightarrow 2H_2 + 2CO$$
$$\Delta H_{298} = 247 \text{ kJ/ mol} \quad (1)$$

The main disadvantage of the dry reforming process is the high rate of carbon formation, this results in the deactivation of catalysts.

*Corresponding author.
E-mail address: meshkani@kashanu.ac.ir (F. Meshkani)

Two main reactions can lead to carbon deposition, mainly, the decomposition of CH_4 (Eq. 2) and carbon monoxide disproportionation (Eq. 3) [5,7-8].

$$CH_4 \leftrightarrow C + 2H_2$$
$$\Delta H^0_{298}=75 \text{ kJ/mol} \quad (2)$$
$$2CO \leftrightarrow C + CO_2$$
$$\Delta H^0_{298} = -172 \text{ kJ/mol} \quad (3)$$

The CRM reaction has been done using several supported metal catalysts such as supported nickel ones [3,9,10]. In addition, nickel catalysts promoted by alkaline and alkaline earth metals were also studied [2,4,5].

The mechanism of the CO_2 reforming of CH_4 was studied extensively to find the precise mechanism details. According to the reported results, there are two main mechanisms: single and double rate determining steps (RDS). In the first mechanism, it is claimed that CH_4 decomposition ($CH_4 \leftrightarrow C+ 2H_2$) is slow, thus, the rate determining step (RDS) is slow [11], while other researchers mentioned the decomposition of CH_xO as

the RDS [12,13]. About the double RDS, the dissociative CH_4 adsorption and CH_xO decomposition are considered as RDS [14,15]. In other reported research, the dissociation of methane and desorption of CO were suggested as the RDS [16]. Furthermore, it is stated that in the Ni/La_2O_3 catalyst, the CH_4 dissociation and the surface carbon species reaction with $La_2O_2CO_3$ are RDS [17]. According to the reported literatures, there are differences in the reforming mechanisms. Due to the different temperatures in reforming studies, the mechanism and the RDS may have been affected considerably [18].

In our previous study, the effect of alkaline earth metals (MgO, CaO and BaO) was investigated over Ni/Al_2O_3 catalysts as support modifiers in CO_2 reforming of methane. The results stated that MgO had the best effect on the catalytic performance and suppressing carbon deposition [4]. The purpose of this work is to study the effect of MgO as a modifier on the kinetic parameters in CRM reaction.

2. Experimental

2.1. Catalyst preparation

Ni/Al_2O_3 and $Ni/MgO\text{-}Al_2O_3$ were synthesized with the method explained in our previous work [4]. In summary, $\gamma\text{-}Al_2O_3$ was employed as a support. This support was prepared by the sol–gel method. $NiN_2O_6.6H_2O$ and $MgN_2O_6.6H_2O$ were used as metal salt precursors. At first, the promoter was added to the support via the simple impregnation method. The modified support was dried at 80 °C and calcined at 700 °C for 4 h. Then, the modified $\gamma\text{-}Al_2O_3$ was impregnated with the appropriate concentration of nickel nitrate to the obtain desired content of nickel. Finally, the impregnated powders were dried at 80 °C overnight and calcined at 500 °C for 4 h.

2.2. Kinetic measurement

Activity measurements were accomplished in a fixed bed quartz micro-reactor at constant temperatures and under ambient pressure. A specific weight of catalyst particles (200 mg) was loaded in the reactor and then reduced in-situ at 600 °C for 4 h in a pure H_2 stream (20 ml/min). Then, the inlet feed containing a mixture of CH_4 and CO_2 was fed into the reactor. For kinetic measurements, the partial pressure dependencies were determined at 650 °C for the reactor test, the feed was composed of CH_4 and CO_2, CH_4: CO_2 =0.25 to 4 by varying the flow rates of CH_4 and CO_2 with a constant total flow rate, which was set by Ar as an inert gas. The effect of H_2 and CO addition was also investigated at 650 °C under the constant CH_4: CO_2=1, while H_2 or CO inlet partial pressures were considered between 0.015 and 0.075 atm. The apparent activation energies were also determined in the range of 550–600 °C and under the CH_4: CO_2 = 1:1. The percentage of reactants and products were determined using a gas chromatograph equipped with a TCD and a Carboxen 1000 column.

2.3. Characterization

X-ray diffraction (XRD) analysis was conducted by an X-ray diffractometer (PANalyticalX'Pert-Pro). The specific surface area was evaluated by the BET method using N_2 adsorption at –196 °C by an automated gas adsorption analyzer (Tristar 3020, Micromeritics). The Barrett, Joyner and Halenda (BJH) method was used to determine the pore size distribution from the desorption branch of the isotherm. Temperature programmed reduction (TPR) experiments were performed using a micrometrics chemisorbs 2750 instrument to investigate the reducibility of the prepared catalysts. In this analysis, 50 mg of the degassed calcined sample was exposed to a heat treatment under a gas stream of 10% H_2 in Ar (30 mL/min).

3. Results and Discussion

3.1. Structural properties of catalysts

The diffraction patterns of the Ni/Al_2O_3 with and without the MgO modifier and $\gamma\text{-}Al_2O_3$ support are displayed in Fig. 1. As shown in the figure, all the samples had the same patterns and after adding MgO modifier to the catalysts, no additional diffraction peaks were detected because of the low percentage of the modifier.

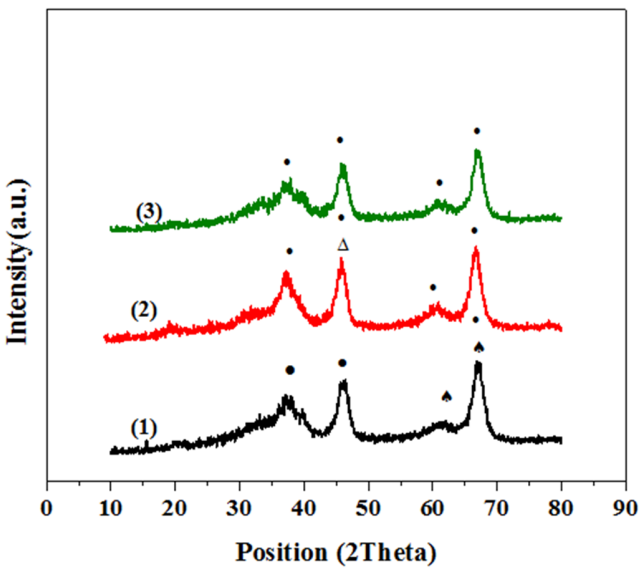

Fig. 1. XRD patterns of: (1) $5\%Ni/Al_2O_3$, (2) $5\%Ni/3\%MgO\text{–}Al_2O_3$, (3) $\gamma\text{-}Al_2O_3$. (●) Al_2O_3, (♠) $NiAl_2O_4$, (Δ) $MgAl_2O_4$.

The observed peaks at 2 θ = 37.2° and 45.9° are assigned to Al_2O_3 (JCPDS Card No. 01- 1303). The peak at 2θ = 62° is ascribed to the $NiAl_2O_4$ phase (JCPDS Card No. 71-0963). The Al_2O_3 and $NiAl_2O_4$ phases are overlapped at 2θ = 67° in the unmodified catalyst. In the MgO modified catalyst, the diffraction peaks of Al_2O_3 phase (JCPDS Card No. 01-1303) were detected at 2θ = 37.1°, 62° and 66.8° whereas $MgAl_2O_4$ (JCPDS Card No. 77-435) and Al_2O_3 (JCPDS Card No. 01-1303) phases are overlapped at 2θ = 45.8°. In the Ni/Al_2O_3 and Ni/MgO-Al_2O3 catalysts the diffraction peaks of NiO phase were not detected. This confirmed that the NiO was highly dispersed on the catalyst carrier, this cannot be identified by the XRD analysis.

The structural properties of γ-Al_2O_3 support, Ni/Al_2O_3 and MgO modified nickel catalysts, are shown in Table 1. As can be seen, the γ-Al_2O_3 support possess high BET area and the MgO-modified catalyst showed lower BET area compared to the unmodified sample. In addition, pore volume of the MgO modified catalyst was lower than that observed for the Ni/Al_2O_3 catalyst due to the block of more pores of the carrier with the addition of modifier. However, the average pore width of the catalysts had no obvious change by adding MgO.

The N_2 adsorption/desorption isotherms and the distributions of pore sizes are displayed in Fig. 2a and 2b, respectively. For both samples, the isotherms can be classified as the class IV with the H2-shaped hysteresis loop, assigned to mesoporous materials [19]. As shown in Fig. 2b, the pore diameter of these two catalysts are between 5 and 17 nm. It is shown that the incorporation of MgO modifier did not considerably affect the pore size distribution.

Temperature-programmed reduction (TPR) patterns of NiO/Al_2O_3 and MgO-modified catalysts are demonstrated in Fig. 3. As can be seen, both samples presented two main reduction peaks. First peak at around 680 ℃is attributed to nickel oxide reduction with high interaction with the catalyst support and the observed peak at higher than 750 ℃ is related to $NiAl_2O_4$ reduction [20-22]. It is seen that the incorporation of MgO into the catalyst support decreased the reduction temperature and increased the reducibility of nickel catalysts.

The kinetic characteristics of the Ni/Al_2O_3 and Ni/MgO-Al_2O_3 in DRM were studied in different functions of CH_4, CO_2, CO and H_2 temperatures and partial pressures.

Table 1. Structural properties of the catalysts with and without MgO, CaO and BaO promoters.

Catalyst	S_{BET} ($m^2.g^{-1}$)	Pore volume ($cm^3.g^{-1}$)	Pore width (nm)	Crystallite size (nm)	
				2θ=46º	2θ=66º
5%Ni/Al_2O_3	173	0.52	8.37	5.23	4.73
5%Ni/3%MgO-Al_2O_3	153	0.44	8.57	14.61	6.61

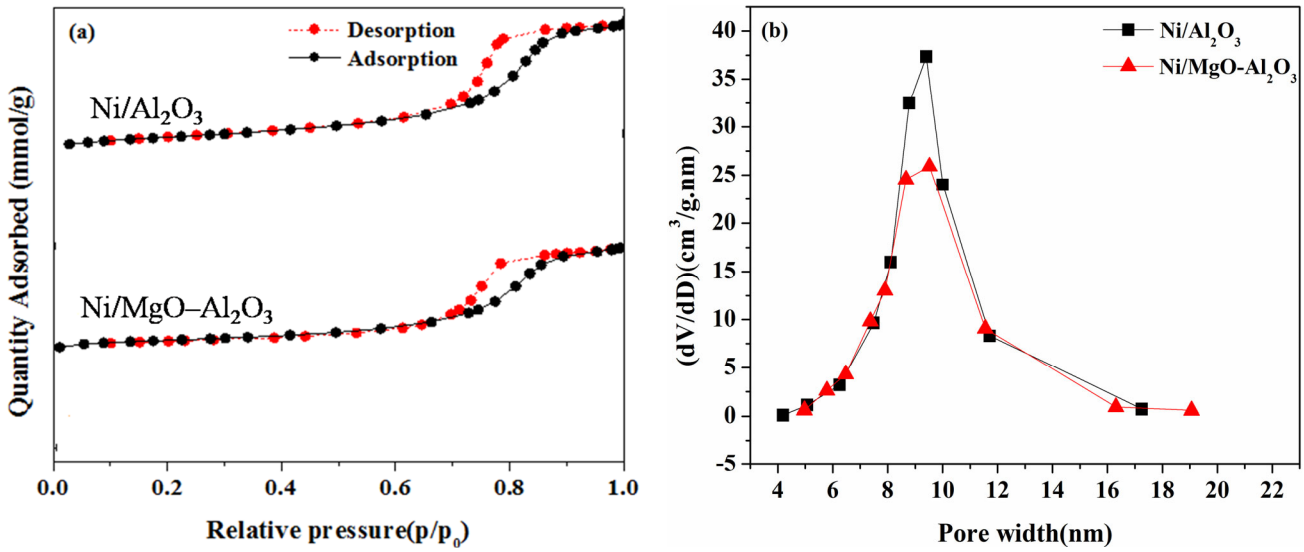

Fig. 2. (a) N_2 adsorption/desorption isotherms. (b) Pore size distributions of Ni/Al_2O_3 and Ni/MgO-Al_2O_3 catalysts.

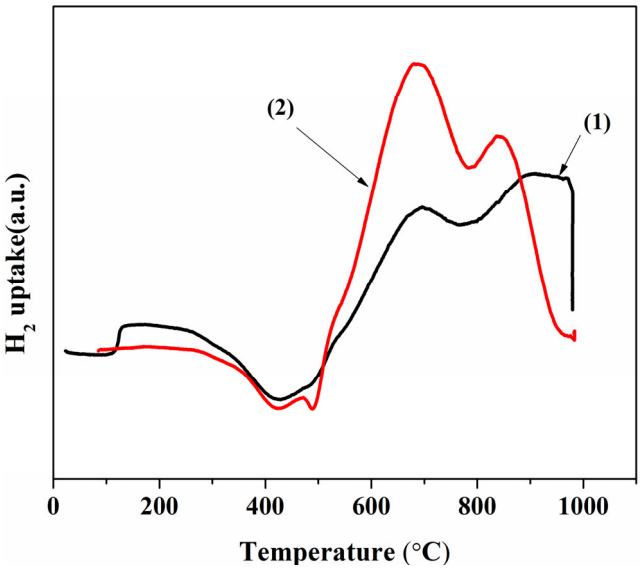

Fig. 3.TPR patterns of (1) Ni/Al_2O_3, (2) $Ni/MgO–Al_2O_3$.

The reaction rates of the catalyst in kinetic measurements, $(-r_{CH_4})$, are determined by the ration of CH_4 conversion to the residence time $(\frac{W_{cat}}{F_{CH_4}})$ as follows (Eq. 4):

$$(-r_{CH_4}) = \frac{X_{CH_4} F_{CH_4}}{W_{cat}} \quad (4)$$

Where X_{CH_4} is CH_4 conversion, F_{CH_4} is the CH_4 flow rate in the feed in ml min^{-1} converted to mmol s^{-1}, W_{cat} is the catalyst weight in g and $(-r_{CH_4})$ is the reaction rate in mmol g^{-1} s^{-1} [14]. A set of experiments were accomplished in order to obtain the X_{CH_4} in DRM. CH_4 consumption rates were calculated by employing the conversion of CH_4 and the Eq. 4, consequently.

In the temperature range of 550-600 °C, the activation energies were determined based on CH_4 and CO_2 consumption rates as CO and H_2 production rates. The Arrhenius plots are shown in Fig. 4 and activation energies calculated from the slopes of plots are presented in Table 2. The activation energy for CH_4 consumption is higher compared to CO_2, this result is in accordance to other values reported in literature [3]. The differences in inactivation energy of the Ni/Al_2O_3 and $Ni/Mg-Al_2O_3$ catalysts may be due to the incorporation of MgO as a support modifier and the resulting changes in the surface mechanism.

3.1. The influence of CH_4 and CO_2 partial pressure on the reaction rate

The influence of the partial pressures of CH_4 and CO_2 on DRM rate was followed over both Ni/Al_2O_3 and $Ni/Mg-Al_2O_3$ catalysts at 1 atm and under different feed rates at 650 °C. In catalytic tests, a constant CH_4 partial pressure of 0.08 atm was used and the partial pressure of CO_2 was between 0.02 and 0.08 atm, contrariwise (Table 4). CH_4 conversion calculated for different CH_4/CO_2 ratios and reaction rates shown in Table 4 were calculated from Eq. 4 for both unmodified and MgO modified samples. The power-low type rate expression applied for the CO_2 reforming of methane is given in Eq. 5:

$$-r_{CH_4} = k(P_{CH_4})^{\alpha}(P_{CO_2})^{\beta} \quad (5)$$

The non-linear regression was applied for the estimation of reaction orders (α and β) and the rate constant (k). In this method, the sum of the squared differences of calculated and experimental CRM reaction rates were minimized using the Levenberg–Marquardt algorithm.

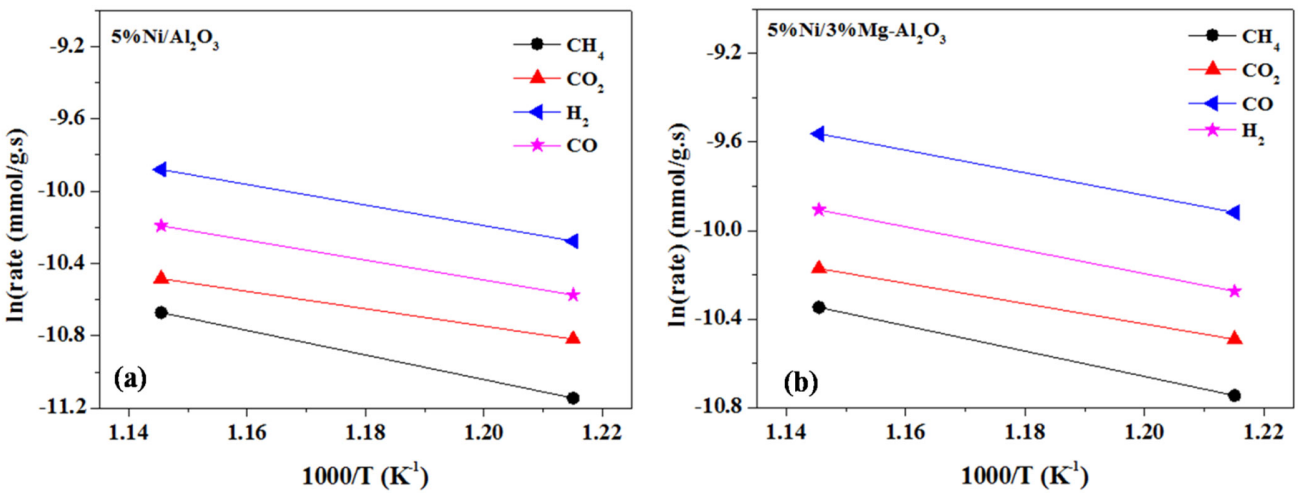

Fig. 4. Arrhenius plots over temperatures ranging between 550 -600°C for (a) Ni/Al_2O_3 and (b) $Ni/MgO-Al_2O_3$ catalysts. Reaction conditions: CH_4/CO_2=1, GHSV= 12000 ($ml.g^{-1}.h^{-1}$).

Table 2. Arrhenius activation energies.

Catalysts	Activation energy E_a(kcal/mol)			
	CH_4	CO_2	CO	H_2
5%Ni/Al_2O_3	13.45	9.52	11.25	10.89
5%Ni/3%Mg-Al_2O_3	11.34	9.09	10.11	10.46

The reaction rates calculated from Eq. 4 are listed in Table 3 for both catalysts.

The reaction orders and the minimum sum of the squared differences of calculated and experimental CRM reaction rates are listed in Table 4.

For both catalysts, the CH_4 reaction order was close to one, Table 4. Furthermore, the CO_2 reaction order was lower than CH_4 for both catalysts, this matter is typical for CRM. Consequently, this result demonstrates that the reaction rate is more sensitive to the CH_4 partial pressure than CO_2 and is in good agreement with the other research [23]. The effect of CH_4 and CO_2 partial pressure on the CH_4 consumption rate is also presented in Figs. 5 and 6. As clearly shown in these figures, the reaction rates were enhanced by increasing partial pressures in the range of 0.02–0.08 atm for both catalysts. Meanwhile, the points show that the results are related to experiments and the lines were fitted to the data points. In addition, the results are related to experiments and the proposed model for each catalyst are in appropriate agreement. Also, the reaction rate relating to the MgO-modified catalyst is higher than that of the Ni/Al_2O_3 sample. This may be due to higher Ni/MgO-Al_2O_3 catalytic activity compared to Ni/Al_2O_3 in CRM [4].

3.2. Effect of CO addition on the CRM rate

For evaluation of the influence of the CO as one of the reaction products on the kinetic expression, CO with different partial pressures in the feed stream (0.015 - 0.075 atm) was considered while the partial pressures of the CO_2 and CH_4 was 0.08 atm at 650 °C. The rate values, considering the CO, are presented in Table 5.

It is shown that CO as a product has a dissuasion role on CH_4 conversion and it is needed to incorporate the CO partial pressure in the expression rate. The DRM reaction rate of CH_4 in the presence of CO is expressed in the power law- type equation and is given in Eq. 6:

$$-r_{CH_4} = k(P_{CH_4})^{\alpha}(P_{CO_2})^{\beta}(P_{CO})^{\delta} \quad \textbf{(6)}$$

Table 3. Reaction rates of CRM at 650°C over Ni/Al_2O_3 and Ni/Mg-Al_2O_3 catalysts.

Partial pressure (atm)		CH_4/CO_2	Reaction rate (mmolg^{-1}s^{-1})	
CH_4	CO_2		5%Ni/Al_2O_3	5%Ni/3%Mg-Al_2O_3
0.02	0.08	0.25	0.026	0.026
0.04	0.08	0.50	0.036	0.039
0.06	0.08	0.75	0.041	0.043
0.08	0.08	1.00	0.044	0.050
0.08	0.06	1.33	0.044	0.050
0.08	0.04	2.00	0.044	0.047
0.08	0.02	4.00	0.031	0.036

Table 4. Estimated reaction orders for unmodified and Mg modified catalysts.

Catalysts	Reaction order		K	σ^2 (mmolg^{-1}s^{-1})^2
	α	β		
5%Ni/Al_2O_3	1.062	0.876	0.170 (mmolg^{-1}s^{-1}atm$^{-1.938}$)	5.996×10^{-6}
5%Ni/3%Mg-Al_2O_3	1.135	0.881	0.196(mmolg^{-1}s^{-1}atm$^{-2.016}$)	1.239×10^{-5}

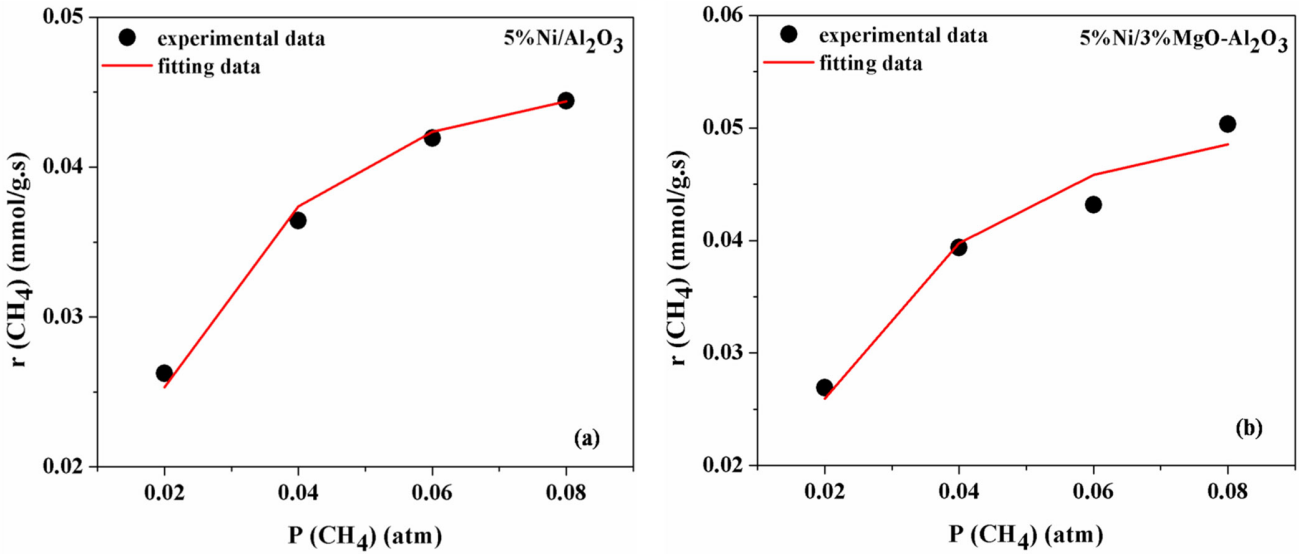

Fig. 5. CH_4 consumption rates as a function of CH_4 partial pressure on the (a) Ni/Al_2O_3 and (b) $Ni/MgO\text{-}Al_2O_3$ catalysts.

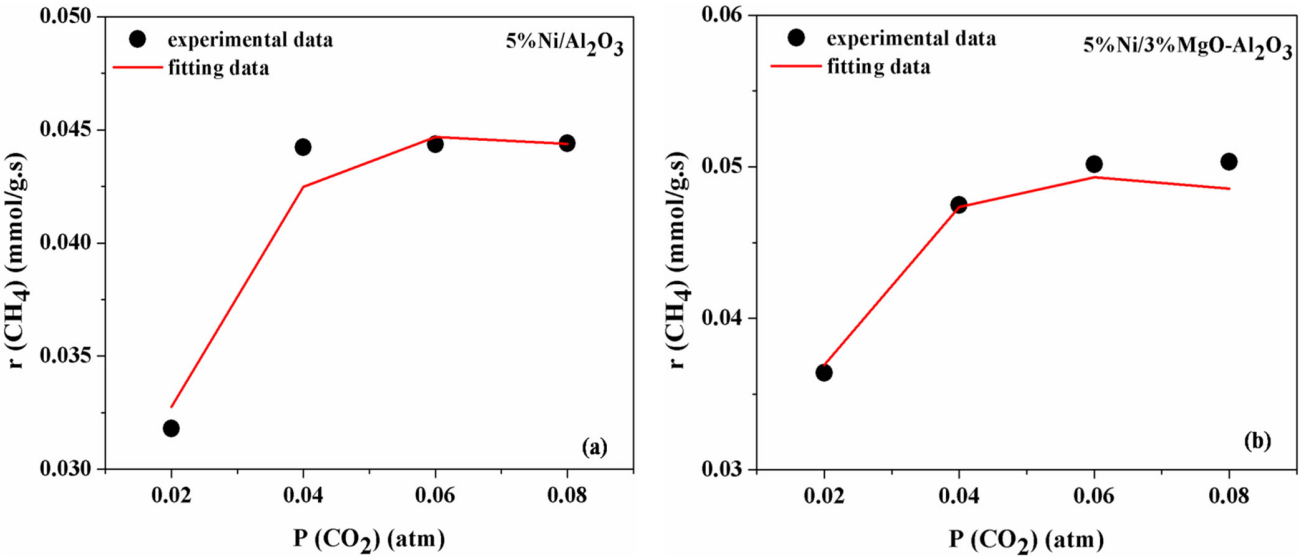

Fig. 6. CH_4 consumption rates as a function of CO_2 partial pressure on the (a) Ni/Al_2O_3 and (b) $Ni/MgO\text{-}Al_2O_3$ catalysts.

Table 5. Effect of CO partial pressure on CRM rate.

Partial pressures (atm)			Reaction rate (mmol/g.s)	
CH_2	CO_2	CO	Ni/Al_2O_3	$Ni/Mg\text{-}Al_2O_3$
0.08	0.08	0.015	0.038	0.038
0.08	0.08	0.030	0.034	0.034
0.08	0.08	0.045	0.032	0.031
0.08	0.08	0.060	0.029	0.030
0.08	0.08	0.075	0.027	0.027

The reaction rate parameters (α, β, δ and k) were determined by using the nonlinear regression technique and the Levenberg–Marquardt algorithm and their values are reported in Table 6 for both catalysts. As can be seen, the presence of CO has a negative effect on the reaction rate in CO_2 reforming of methane due to adsorption of CO on the active centers where it decomposes into activated surface oxygen and carbon. This activated carbon covers the active sites and decreases the catalytic activity and the reaction rates [3]. Also, the reaction rates versus CO partial pressure were plotted in Fig. 7. CH_4 consumption decreased as the CO partial pressure increased in the CRM reaction.

3.3 Effect of H_2 addition on the CRM rate

The effect of hydrogen of the feed on the CRM rate was also investigated in the range of 0.015 to 0.075 atm while CH_4 and CO_2 were kept fixed at 0.08 atm at 650 ℃ and the results are presented in Table 7. According to this table, addition of H_2 has a negative effect on the reaction rate for both catalysts in CO_2 reforming of CH_4. The power-law type rate expression applied for the dry reforming of CH_4 in the presence of H_2 is given in Eq. 7:

$$-r_{CH_4} = k(P_{CH_4})^{\alpha}(P_{CO_2})^{\beta}(P_{H_2})^{\delta} \quad (7)$$

Table 6. Estimated reaction rate parameters in the presence of CO.

Catalysts	Reaction order of CO (δ)	k	Power-type rate law
5%Ni/Al_2O_3	-0.223	2.981	$-r_{CH_4}=k(P_{CH_4})^{1.062}(P_{CO_2})^{0.876}(P_{CO})^{-0.223}$
5%Ni/3%Mg-Al_2O_3	-0.224	0.102	$-r_{CH_4}=k(P_{CH_4})^{1.135}(P_{CO_2})^{0.881}(P_{CO})^{-0.224}$

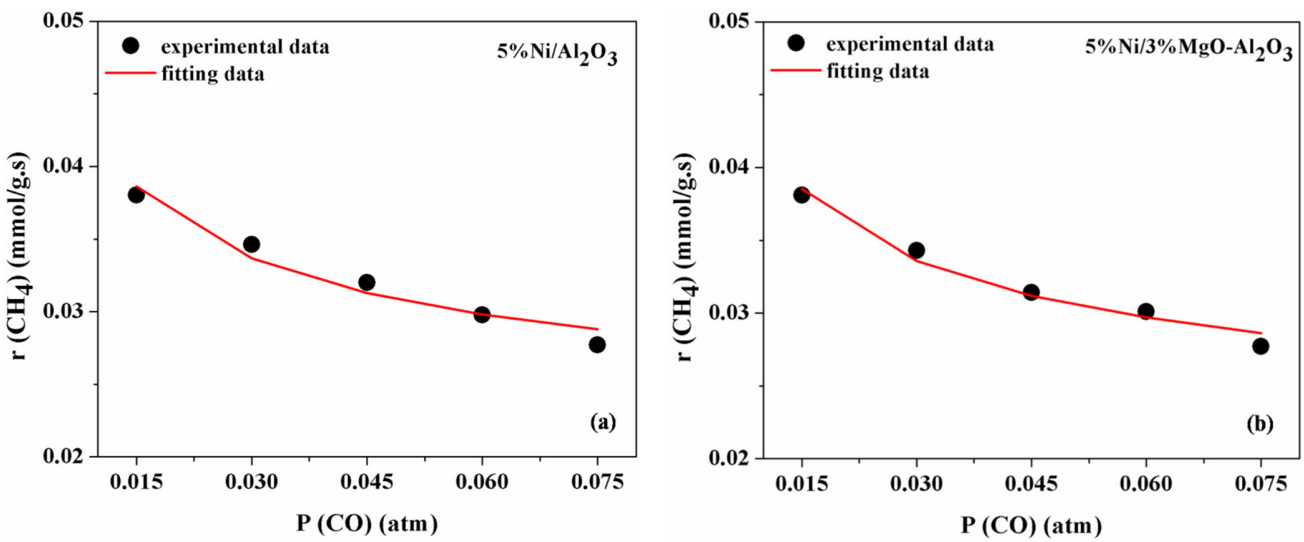

Fig. 7. CH_4 consumption rates as a function of CO partial pressure on the (a) Ni/Al_2O_3 and (b) Ni/MgO-Al_2O_3 catalysts.

Table 7. Effect of H_2 partial pressure on CRM rate.

Partial pressures (atm)			Reaction rate (mmol/g.s)	
CH_4	CO_2	H_2	Ni/Al_2O_3	Ni/Mg-Al_2O_3
0.08	0.08	0.015	0.033	0.033
0.08	0.08	0.030	0.026	0.027
0.08	0.08	0.045	0.021	0.022
0.08	0.08	0.060	0.017	0.018
0.08	0.08	0.075	0.013	0.014

The reaction rate parameters (α, β, δ and k) were determined using the nonlinear regression technique and the Levenberg–Marquardt algorithm and their values are reported in Table 8 for both catalysts.

Also, CH_4 consumption rates in the presence of H_2 were shown as a function of partial pressure of hydrogen in Fig. 8. After addition of hydrogen to the feed, the rate of methane conversion rate initially declined for both samples.

3.4. Surface reaction models

In this part, other CO_2 kinetics methods of CH_4 reforming are expressed, because the power-law model was investigated in the previous section, may be insufficient, due to its simplicity in application and the wide range of partial pressures. Different types of reaction modes are proposed in the literature such as Langmuir Hinshelwood (LH), Eley- Rideal (ER) and Hougen-Watson (HW) [23-30]. To investigate the effect of MgO modifier on the reaction kinetics of the Ni catalyst, the experimental CH_4 consumption rates for both Ni/Al_2O_3 and $Ni/Mg\text{-}Al_2O_3$ were fitted to some kinetic type models, Table 9. The model made a distinction on the basis of the variance value and/or physical meanings of presented constants. The models which presented negative parameter values or poor correlation coefficients was not considered. The variance of the experimental error (δ^2) for each model was compared and the equation that was closest to the experimental data was determined and finally the equation with a smaller variance was selected.

The main assumptions of the models mentioned in this study are summarized in following. In model 1, the kinetic of the Ir/Al_2O_3 catalyst in DRM is studied based on Eley- Rideal model and it was assumed that CO_2 is adsorbed on the catalyst surface in adsorption equilibrium [29]. It is mentioned that the rate-determining step (slow step) is the reaction of adsorbed CO_2 with CH_4 from the gas phase leading directly to products. The model 2 is suggested for Ni/Al_2O_3 [24]. It is claimed that CH_4 is decomposed to hydrogen and active carbon. Then, 2CO is produced through the reaction between active carbon and CO_2. Hence, the CO formation is the slow step (rate-determining step). In the model 3, the rate of reaction expressed based on the Langmuir Hinshelwood model assuming CH_4 decomposition is the slow step [25].

Table 8. Estimated reaction rate parameters in the presence of H_2.

Catalysts	Reaction order of H_2 (δ)	K	Power-type rate law
$5\%Ni/Al_2O_3$	-0.567	1.147	$-r_{CH_4}=k(P_{CH_4})^{1.062}(P_{CO_2})^{0.876}(P_{H_2})^{-0.567}$
$5\%Ni/3\%Mg\text{-}Al_2O_3$	-0.536	0.042	$-r_{CH_4}=k(P_{CH_4})^{1.135}(P_{CO_2})^{0.881}(P_{H_2})^{-0.536}$

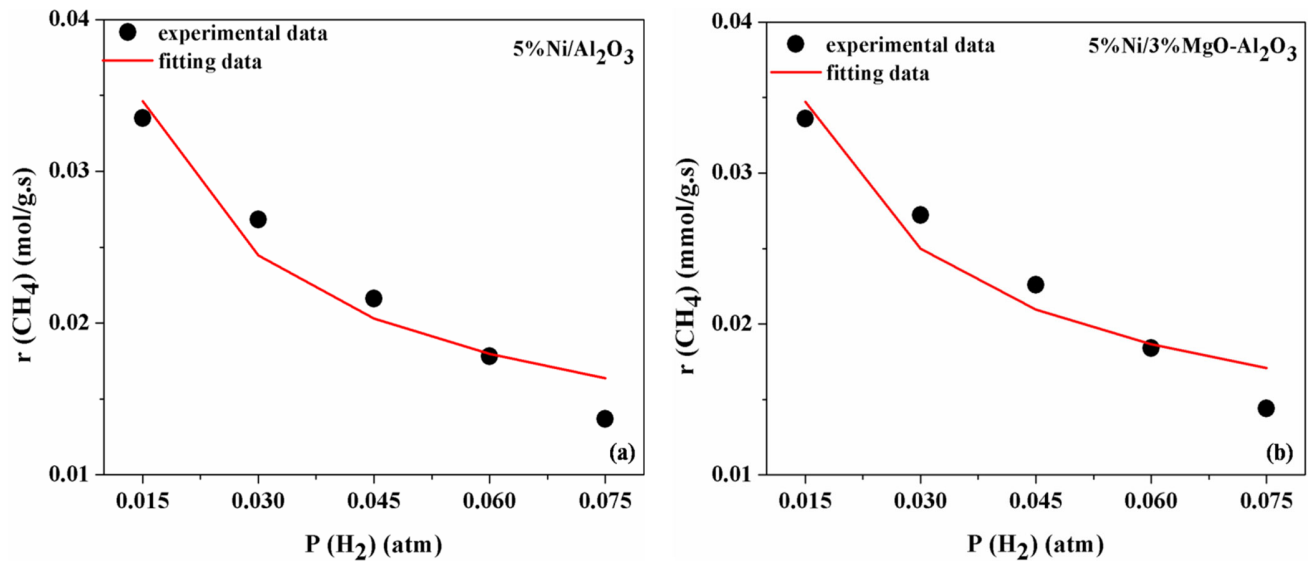

Fig. 8. CH_4 consumption rates as a function of H_2 partial pressure on the (a) Ni/Al_2O_3 and (b) $Ni/MgO\text{-}Al_2O_3$ catalysts.

Table 9. Langmuir–Hinshelwood (LH) type rate expressions.

Model number	Reaction rate
1	$(-r_{CH_4}) = \frac{kK_{CO_2}P_{CH_4}P_{CO}}{(1 + K_{CO_2}P_{CO_2})}$
2	$r_{CH_4} = \frac{k_1P_{CH_4}P_{CO_2}}{(1 + K_1P_{CH_4})(1 + K_2P_{CO_2})}$
3	$r = \frac{aP_{CH_4}P_{CO_2}^2}{(P_{CO_2} + bP_{CO_2}^2 + cP_{CH_4})^2}$
4	$(-r_{CH_4}) = \frac{kK_{CO_2}K_{CH_4}P_{CH_4}P_{CO_2}}{(1 + K_{CO_2}P_{CO_2} + K_{CH_4}P_{CH_4})^2}$
5	$(-r_{CH_4}) = \frac{kP_{CO_2}P_{CH_4}}{(1 + K_1P_{CH_4} + K_2P_{CO})(1 + K_3P_{CO_2})}$
6	$(-r_{CH_4}) = \frac{kK_{CO_2}P_{CH_4}P_{CO_2}}{(1 + K_{CO_2}P_{CO_2} + K_{CO}P_{CO})}$
7	$(-r_{CH_4}) = \frac{kK_{CH_4}P_{CH_4}P_{CO_2}^m}{(1 + K_{CH_4}P_{CH_4})}$
8	$(-r_{CH_4}) = \frac{kP_{CH_4}^mP_{CO_2}^n}{(1 + K_{CO_2}P_{CO_2} + K_{CO}P_{CO} + K_{CH_4}P_{CH_4})}$

The Langmuir Hinshelwood model was also studied by Mark et al. [29]. In this model, it is mentioned that both reactants (CH_4 and CO_2) are adsorbed and H_2 and CO are produced by the surface reaction between them; this is the rate determining step. Richardson and Paripatyadar [30] reported the terminate equation. Olsbye et al. [26] studied a Langmuir Hinshelwood model type (model 5) over $Ni/La/Al_2O_3$ and also the effect of CO on the CH_4 consumption rate i. In model 6 that was derived from the model 1, the preventing effect of CO is considered in the equation. Olsbye et al. [26] and Mark et al., [29] represented a Eley–Rideal model type (model 7) assuming the reaction between CH_x and $CO_{2,\,g}$ is the slow step. In this model, the adsorbed CH_4 on the surface of the catalyst dissociates to CH_x and H. The reaction of adsorbed CH_x with CO_2 from the gas phase is the rate-determining step. In addition, the preventing effects of both CO and CH_4 is considered in model 8.

The adsorption constants of CRM for Ni/Al_2O_3 and $Ni/Mg\text{-}Al_2O_3$ catalysts are presented in Table 10. The results show that models 1, 4, 6 and 7 with unmodified catalyst and models 1, 3, 4, 6 and 7 for the MgO modified catalyst give physically meaningful values. The lowest squared error for Ni/Al_2O_3 was observed in the model 5 and 6 implying that the adsorption of CH_4 is weak and the surface coverage of CH_4 is low for Ni/Al_2O_3 at the studied pressures; which means that this model is the best model for presenting the behavior of the Ni/Al_2O_3 catalyst; while for $Ni/Mg\text{-}Al_2O_3$, the model 6 presents the lowest squared error and the proposed models are the best to describe the reaction rate.

4. Conclusions

Ni/Al_2O_3 and $Ni/MgO\text{-}Al_2O_3$ catalysts were prepared and employed in CO_2 reforming of CH_4. The structural properties of the catalysts represented that the addition of MgO modifier to the catalyst decreased the specific surface area and pore volume. Moreover; the reduction temperature decreased in MgO modified catalyst; this leads to improve the reducibility of nickel catalyst compared to the unmodified catalyst. The kinetics of the dry reforming were studied over the prepared samples. The activation energy was calculated from the Arrhenius plot. The result demonstrated that the activation energy for CH_4 consumption is higher than CO_2. The CH_4 consumption rate parameters were expressed by the power-law model and the results showed that the reaction rate was more sensitive to CH_4 partial pressure compared to CO_2, it caused the order of reaction for CH_4 becomes bigger than the CO_2. Also, the reaction rate for the MgO- modified catalyst was higher

Table 10. Model parameters obtained for Ni/Al_2O_3 and $Ni/Mg\text{-}Al_2O_3$.

Catalysts	Model	Rate parameters	$\sigma^2(mmolg^{-1}s^{-1})^2$
Ni/Al_2O_3	1	k=8.978 mmol/g.s.atm K_{CO_2}=0.179 atm	11.3×10^{-4}
	4	k=0.185 $mmolg^{-1}s^{-1}$ K_{CO_2}=975 atm^{-1} K_{CH_4}=770atm^{-1}	2.1×10^{-6}
	5	k=5.186 $mmolg^{-1}s^{-1}atm^{-2}$ K_1=1.964 atm^{-1} K_2=2.051 atm^{-1} K_3=6.688 atm^{-1}	1.3×10^{-6}
	6	k = 18.478 $mmolg^{-1}s^{-1}atm^{-1}$ K_{CO_2}= 0.383atm^{-1} K_{CO}=1.826 atm^{-1}	1.3×10^{-6}
	7	k=536 $mmolg^{-1}s^{-1}$ K_{CH_4}=$298\times10^{-8}atm^{-1}$ m=0.008 atm^{-1}	8.1×10^{-6}
$Ni/Mg\text{-}Al_2O_3$	1	k=9.886 mmol/g.s.atm K_{CO_2}=0.197 atm	8.6×10^{-4}
	4	k=39.732 $mmolg^{-1}s^{-1}$ K_{CO_2}=0.367atm^{-1} K_{CH_4}=0.018atm^{-1}	7.1×10^{-7}
	6	k = 18.343 $mmolg^{-1}s^{-1}atm^{-1}$ K_{CO_2}= 0.381atm^{-1} K_{CO}=1.744 atm^{-1}	5.9×10^{-7}
	7	k=2.657 $mmolg^{-1}s^{-1}$ K_{CH_4}=$60.177\times10^{-7}atm^{-1}$ m=0.007 atm^{-1}	1.5×10^{-6}

than the unmodified sample. This may be due to higher catalytic activity of Ni/MgO-Al_2O_3 compared to Ni/Al_2O_3 in CRM. Moreover, the effect of adding CO and H_2 in the CRM rate were studied. The results show that the H_2 and CO have the preventing and negative effects on the reaction rate in the dry reforming of CH_4. Some kinetic type models were proposed in order to investigate the effect of MgO modifier on the reaction kinetics of the Ni catalyst and the best models presenting the behavior of the modified and unmodified catalyst were selected.

Acknowledgments

The authors are grateful to University of Kashan for supporting this work by Grant No. 158426/16.

References

[1] L. Xu, H. Song, L. Chou, Appl. Catal. B 108-109 (2011) 177-190.
[2] Z. Alipour, M. Rezaei, F. Meshkani. J. Ind. Eng. Chem. 20 (2014) 2858-2863.
[3] Ş. Özkara-Aydınoğlu, A.E. Aksoylu, Chem. Eng. J. 215-216 (2013) 542-549.
[4] Z. Alipour, M. Rezaei, F. Meshkani, Fuel 129 (2014) 197-203.
[5] Z. Alipour, M. Rezaei, F. Meshkani, J. Energ. Chem., 23 (2014) 633-638.
[6] F. Mirzaei, M. Rezaei, F. Meshkani, Z. Fattah, J. Ind. Eng. Chem. 21 (2015) 662-667.
[7] M. Khajenoori, M. Rezaei, F. Meshkani, J. Ind. Eng. Chem. 21 (2015) 717-722.
[8] N. Hadian, M. Rezaei, Z. Mosayebi, F. Meshkani, J. Nat. Gas. Chem. 21 (2012) 200-206.
[9] A.S.A. Al-Fatesh, A.H. Fakeeha, A.E. Abasaeed, Chin. J. Catal. 32 (2011) 1604-1609.
[10] X. Yu, N. Wang, W. Chu, M. Liu, Chem. Eng. J. 209 (2012) 623-632.
[11] J. Wei, Iglsia, J. Catal. 224 (2004) 370-383.
[12] J.Z. Luo, Z.L. Yu, C.F. Ng, C.T. Au, J. Catal. 194 (2000) 198-210.
[13] T. Osaki, T. Mori, J. Catal. 204 (2001) 89-97.
[14] M.C.J. Bradford, M.A. Vannice, Appl. Catal. A 142 (1996) 97-122.
[15] A. Nandini, K.K. Pant, S.C. Dhingra, Appl. Catal. A. 308 (2006) 119-127.
[16] L.M. Aparicio, J. Catal. 165 (1997) 262-274.
[17] V.A. Tsipouriari, X.E. Verykios, Catal. Today 64 (2001) 83-90.
[18] Y. Cui, H. Zhang, H. Xu, W. Li, Appl. Catal. A 318 (2007) 79-88.
[19] G. Leofanti, M. Padovan, G. Tozzola, B. Venturelli, Catal. Today 41 (1998) 207-219.
[20] K. Sutthiumporn, S. Kawi, Int. J. Hydrogen Energy 36 (2011) 14435-14446.
[21] H.S. Hyun-Seog Roh, K.W. Jun, Catal. Surv. Asia 12 (2008) 239-252.
[22] M. García-Diéguez, C. Herrera, M.Á. Larrubia, L.J. Alemany, Catal. Today 197 (2012) 50-57.
[23] P. Ferreira-Aparicio, A. Guerrero-Ruiz, I. Rodríguez-Ramos, Appl. Catal. A 170 (1998) 177-187.
[24] S. Wang, GQA. Lu, Ind. Eng. Chem. Res. 38 (1999) 2615-2625.
[25] Z.L. Zhang, X.E. Verykios, Catal. Today 21 (1994) 589-595.
[26] U. Olsbye, T. Wurzel, L. Mleczko, Ind. Eng. Chem. Res. 36 (1997) 5180-5188.
[27] J.F. Munera, S. Irusta, L.M. Cornaglia, E.A. Lombardo, D.V. Cesar, M. Schmal, J. Catal. 245 (2007) 25-34.
[28] T. Osaki, H. Fukaya, T. Horiuchi, K. Suzuki, T. Mori, J. Catal. 180 (1998) 106-109.
[29] F.M. Mark, F. Mark, W.F. Maier, Chem. Eng. Technol. 20 (1997) 361-370.
[30] J.T. Richardson, S.A. Paripatyadar, Appl. Catal. 61 (1990) 293-309.